

4. Davis, D. W., Walker, M., Takashi, M. and Masaki, T., *Sadhana*, 2003 (in press).
5. Taniguchi, N., *Precis. Eng.*, 1994, **16**, 5–24.
6. Miyashita, M., 'Brittle/ductile machining', Fifth International Seminar on Precision Engineering Monterey, CA, USA, 1989.
7. Venkatesh, V. C., Chee, W. K., Pey, K. L., Tan, K. H. and Trigg, A., 'Surface integrity of polished infra-red optics and glass', Proceedings of 11 American Society of Precision Engineering Conference, Monterey, CA, USA, 1996, Vol. 14, pp. 490–495.
8. Schinker, M. G., *J. Precis. Eng.*, 1991, **13**, 208–218.
9. Bifano, T. G., DePiero, D. K. and Gollini, D., *J. Precis. Eng.*, 1983, **15**, 238–247.
10. Tan, C. P., CNC rough grinding of aspheric surfaces, B Eng (Mech.) Thesis, National University of Singapore, 1984.
11. Ang, K. W., Economic analysis of aspheric surface grinding using 4 and 5 axes generation on vertical machining CNC Centres, M S Thesis, Tennessee Technological University, 1989.
12. Tan, C. P., Aspheric surface grinding and polishing of thermal imaging materials, M S Thesis, Tennessee Technological University, 1990.
13. Russell, R. G., Comparison of metal and resinoid bonded grinding wheels with various grit sizes in the aspheric surface generation of silicon lenses, M S Thesis, Tennessee Technological University, 1993.
14. Kapoor, A., A study on mechanisms of aspheric grinding of silicon, M S thesis, Tennessee Technological University, 1993.
15. Zhong, Z. and Venkatesh, V. C., *Ann. CIRP*, 1994, **43**, 323–326.
16. Venkatesh, V. C. and Silva, D., 'On the wear of diamond tools in numerical control contour generation', Proceedings of International Conference on Optimum resources utilisation through tribo-tetro-technology, New Delhi, India, 1981, pp. J2. 1–8.
17. Blake, P. N., Ductile-regime turning of Ge and Si, Ph D Thesis, North Carolina State University, Raleigh, 1988.
18. Venkatesh, V. C. and Izman Sudin, 'Novel diamond wheel for fine finishing of I. C. chip packaging material for failure analysis and for machining small areas in brittle materials like silicon and glass', Invention disclosure made on 18 March 2002, University Technology Malaysia, Johor Bahru, Malaysia, 2002.
19. Venkatesh, V. C. and Izman Sudin, Application for Malaysian Patent for above invention filed on 30 January 2003. No. PI 20030326.

Received 30 August 2002; revised accepted 3 April 2003

First evidence for anomalous thick crust beneath mid-Archean western Dharwar craton

Sandeep Gupta[†], S. S. Rai^{†*}, K. S. Prakasam[†], D. Srinagesh[†], R. K. Chadha[†], Keith Priestley[‡] and V. K. Gaur[#]

[†]National Geophysical Research Institute, Hyderabad 500 007, India

[‡]Bullard Laboratories, University of Cambridge, Cambridge, CB3 0EZ, UK

[#]Indian Institute of Astrophysics, Bangalore 560 034, India

We report an anomalous present day crustal thickness of 43–52 km beneath the 3.4–3.0 Ga mid-Archean segment of the western Dharwar craton (WDC) undisturbed by Proterozoic events. In contrast, adjoining late-Archean (2.7–2.5 Ga) eastern Dharwar craton (EDC) has a 33–40 km crustal thickness similar to the Archean global average. Considering that mineral assemblages in the central part of the WDC crust (amphibolite grade metamorphics) equilibrated at a depth of 15–20 km, we argue that the western Dharwar crust 3.0 Ga ago must have been at least 60–80 km thick. Both segments of Dharwar craton crust

exhibit Poisson's ratio of 0.24–0.28 suggesting felsic to intermediate average crustal composition. The thickest crust beneath WDC has also underlying high-velocity thicker lithosphere compared to EDC, inferred from faster arrivals of teleseismic P and S wave. The contact between WDC and EDC is marked as gradational thinning of crust (42–36 km) from Chitradurga thrust to the western part of Closepet granite. In WDC, the crustal thickness increases in step fashion towards the oldest crustal block. These details suggest terrain accretion in Dharwar craton during 3.4 to 2.5 Ga through subduction related process.

THE origin and growth of the Archean crust is a subject of intense investigation. The geological, geochemical and geophysical observations suggest a fundamental difference between early- and mid-Archean crust with those

evolved during and subsequent to the late Archean¹. Our understanding about the nature of the early crust and its possible variation through geological time remains incomplete due to insufficient knowledge about the thickness and composition of the undeformed early- and mid-Archean crust. Global review of seismological data^{2,3} suggests that the Precambrian shields have an average

*For correspondence. (e-mail: srrai_ngri@rediffmail.com)

crustal thickness of 37 ± 5 km and P-velocity of 6.4 km/s. Also, Durrheim and Mooney⁴ observed thicker and mafic crust beneath the Proterozoic terrain than beneath the Archean. Recent analysis of broadband wave-forms using receiver function⁵⁻⁷ suggests bi-modal distribution of V_p/V_s (1.74, 1.82) for the Archean terrains. Rudnick and Fountain³ and Christensen⁸ argue for intermediate composition of the average crust with Poisson's ratio $s = 0.265$. For common rock types, s varies from 0.20 to 0.35. Higher silica content lowers s , while the higher mafic content increases it. For lower crustal rocks, low s (< 0.26), intermediate s (0.26–0.28) and high s (> 0.28) characterize its felsic, intermediate and mafic composition⁹.

To investigate the crust and mantle structure beneath the Dharwar craton, we operated temporary broadband seismic stations during 1999–2001. The earthquake wave-forms were recorded at 20 sps using broadband CMG3T/3ESP sensors and REFTEK data loggers. The location of these stations is depicted in Figure 1.

We present here evidence for the thickest undisturbed mid-Archean crust with a felsic to intermediate composition in western Dharwar craton through receiver function analysis of earthquake wave-forms from teleseismic dis-

tance recorded over the network of broadband seismic stations. Along with the crustal character, we also investigate the lithospheric properties underlying the craton to constrain the process responsible for the growth of the crust in Dharwar craton during the Archean.

Tectonic setting

The Dharwar craton (Figure 1) is one of the major Archean blocks of the Indian subcontinent. Detailed geology is presented in several publications¹⁰⁻¹². Geochronological and geochemical studies suggest > 3.4 – 3.0 Ga continental nucleus in the western part of the Dharwar craton^{13,14} wrapped by 2.7–2.5 Ga crustal blocks to the east. Major rock types of the craton include gniesses, schist belts and diapiric trondhjemites. The craton is divided into western and eastern craton by a N–S elongated 2.5 Ga Closepet granite. However, an alternative line of contact between EDC and WDC is proposed to be the Chitradurga thrust, parallel to and ~ 50 km west of the Closepet granite. The actual boundary between the two cratonic blocks remains debatable. The western Dharwar craton (WDC) was formed through accretion of terrains¹⁴ evolved from the mantle over a period > 3.4 to 3.0 Ga. The > 3.4 Ga-old 'nucleus' is a major low strain zone in the craton protected by the severity of compressive deformation¹⁵. The Dharwar craton primarily has tholeiitic and picritic composition. The mafic–ultramafic (komatiites) complexes have been reported from Gorur, Hassan region in WDC and Kolar in EDC. The eastern Dharwar craton (EDC) crust contains granitoid rocks, all juvenile addition to the continental crust during 2.6–2.5 Ga¹⁶. The EDC also hosts diamondiferous kimberlite pipes (Figure 1). These diamonds, which are yet to be dated, occur in kimberlites of Proterozoic (1100 Ma) age. To the south, the Dharwar craton passes through narrow gradational zone and into the high-grade metamorphic (2.6 Ga) terrain, while to the east it is wrapped by the Proterozoic Cuddapah basin (CB) and the eastern ghat granulite terrain (EGGT). The evolutionary history of Cuddapah basin¹⁷ could be traced back to the first igneous activity in the form of lava flow at about 1850 Ma in the SW part of the basin adjoining EDC.

Receiver function and crustal structure

A teleseismic P-wave propagating to a seismic station generates converted S waves at boundaries with significant impedance contrast beneath the station (Figure 2). Moho is one such most significant boundary. Receiver functions (RF) are wave-forms computed by deconvolving vertical component from the radial/tangential components to isolate the converted phases from coda of the P waves. It contains information related to P and converted and reflected S waves from the seismic discontinuities in the crust and the mantle. We follow an approach using spectral

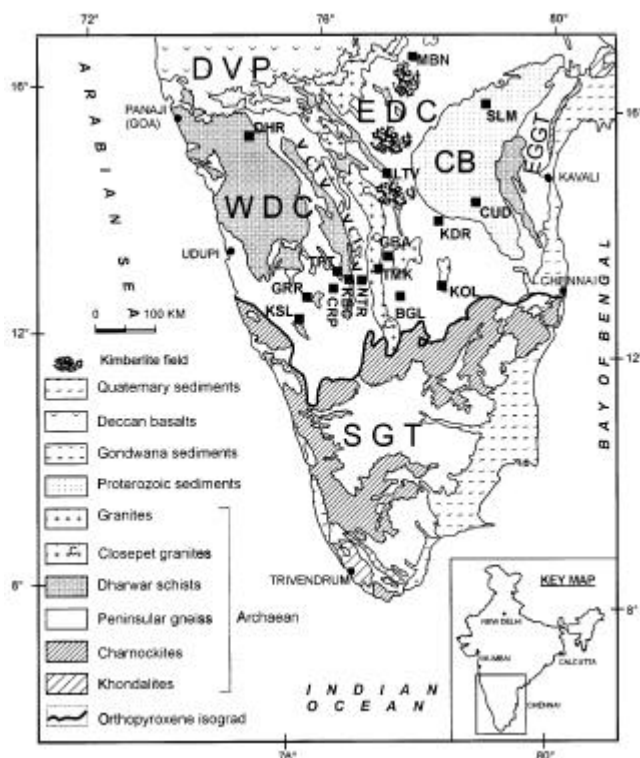


Figure 1. Map showing the principal segments of Dharwar craton and adjoining geological provinces in South India: WDC – western Dharwar craton, EDC – eastern Dharwar craton, CB – Cuddapah basin, EGGT – eastern ghat granulite terrain, SGT – southern granulite terrain, DVP – Deccan volcanic province, CG – Closepet granite, CT – Chitradurga thrust. Locations of broadband seismic stations are shown as black squares.

division deconvolution¹⁸ to compute receiver functions. The Moho P to S converted wave (P_s) is most dominant on the radial RF and arrives in the time window 4–7 s after the P. In this study, we used earthquake waveforms from teleseismic distances (30° – 95°) recorded over broadband seismic stations in Dharwar craton. Receiver functions were computed at each station for individual earthquakes and stacked in narrow azimuth and delta range to improve S/N ratio. Stacked radial receiver function for individual station shows remarkable spatial coherence of Moho converted P_s phase with the surface geology and compositional boundaries (Figure 3). P_s –P travel time in the EDC is 3.9–4.52 s while in the WDC it varies from 5.32 to 5.91 s indicating significant variation in crustal thickness/Poisson's ratio. Maximum P_s –P time separation is observed over the oldest crustal block (~ 3.4 Ga) at GRR. P_s –P time is dependent on average crustal thickness (H), V_p and V_p/V_s . However, Zandt *et al.*¹⁹ showed that this time difference is dependent more on H than on other parameters. A P-wave velocity variation over 10% (6.0–6.6 km/s) can change the thickness estimate by ~ 3 km.

To quantify the crustal thickness and Poisson's ratio in the vicinity of each station, we modelled the amplitude and travel times of P to S conversions at the Moho (P_s) and its crustal multiples (P_pP_{ms} and $P_pS_{ms} + P_sP_{ms}$) in the radial receiver function²⁰. For a large number of crustal models with varying thicknesses H (25–60 km) and varying V_p/V_s (1.6–1.8), we compute corresponding arrival times of P_s , P_pP_{ms} and $P_pS_{ms} + P_sP_{ms}$ (say t_1 , t_2 and t_3) and stack the amplitude of RF through the equation:

$$S(H, V_p/V_s) = w_1 r(t_1) + w_2 r(t_2) - w_3 r(t_3)$$

where $r(t)$ is the radial receiver function and w_i the weights assigned to RF at time t_i . Since crustal multiples are relatively weak signals compared to conversion, Zhu and Kanamori²⁰ proposed weightage of 0.7, 0.2 and 0.1 respectively for amplitudes at times t_1 , t_2 and t_3 . The H and V_p/V_s providing the maximum amplitude in S is considered the best approximation.

The method requires *a priori* knowledge of the average crustal P velocity. Recently, Sarkar *et al.*²¹ modelled an earlier Kavali–Udipi deep seismic profile measurements²² across Dharwar craton and inferred a simple two-layer crust with velocity 6.1 km/s for the upper crust (23 km) and 6.9 km/s for the lower crust in both segments of the craton. The inferred Moho depth is ~ 35 km for the EDC and 40 km for the WDC. We computed the average crustal thickness and V_p/V_s for individual station using stacked receiver function from events in the same azimuth and distance range ($\pm 5^\circ$) using the above equation considering an average 6.45 km/s P-wave crustal velocity. Figure 4 details the H and V_p/V_s computation for a few broadband stations. Detailed result for individual station is presented in Table 1. To assess the reliability of our H and V_p/V_s values, we compared the result with those of

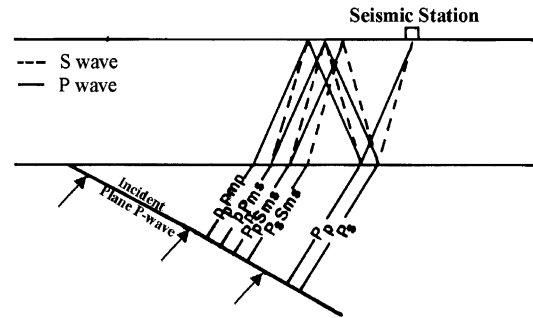


Figure 2. Ray paths for converted P_s phase and major multiples for a simple layer over a half-space model.

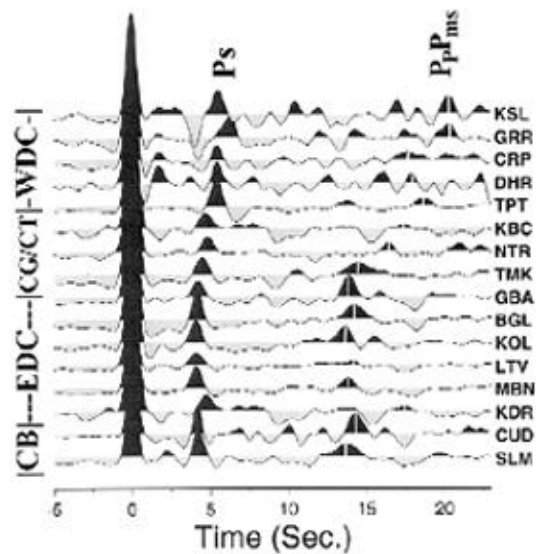


Figure 3. Stacked radial receiver function for stations in Dharwar craton grouped according to their geological/structural proximity. Note the increase in P_s time for stations in western Dharwar craton. P_pP_{ms} phase is also marked for individual station.

Rai *et al.*²³ for common stations like GBA, BGL, LTV and MBN. The two results agree very well with an accuracy of 1 km for H and 0.01 for V_p/V_s .

Crustal composition

Examination of Table 1 suggests that stations in both the EDC and WDC exhibit Poisson's ratio in the range of 0.24–0.28. These values are lower than the Archean crust global average⁵ of 0.29 ± 0.02 and are in better agreement with Last *et al.*⁶ and Kumar *et al.*²⁴ suggesting a more felsic/intermediate crustal composition beneath Dharwar craton. This is also supported by the absence of > 7.0 km/s lower crust P-wave velocity in both EDC and WDC from modelling of DSS wave-form data. The other evidence to support our inferred felsic/intermediate crustal composition includes high ($> 60\%$) SiO_2 content²⁵ and low P velocity²⁶ (6.0–6.5 km/s) in the metamorphic rocks of southern granulite terrain.

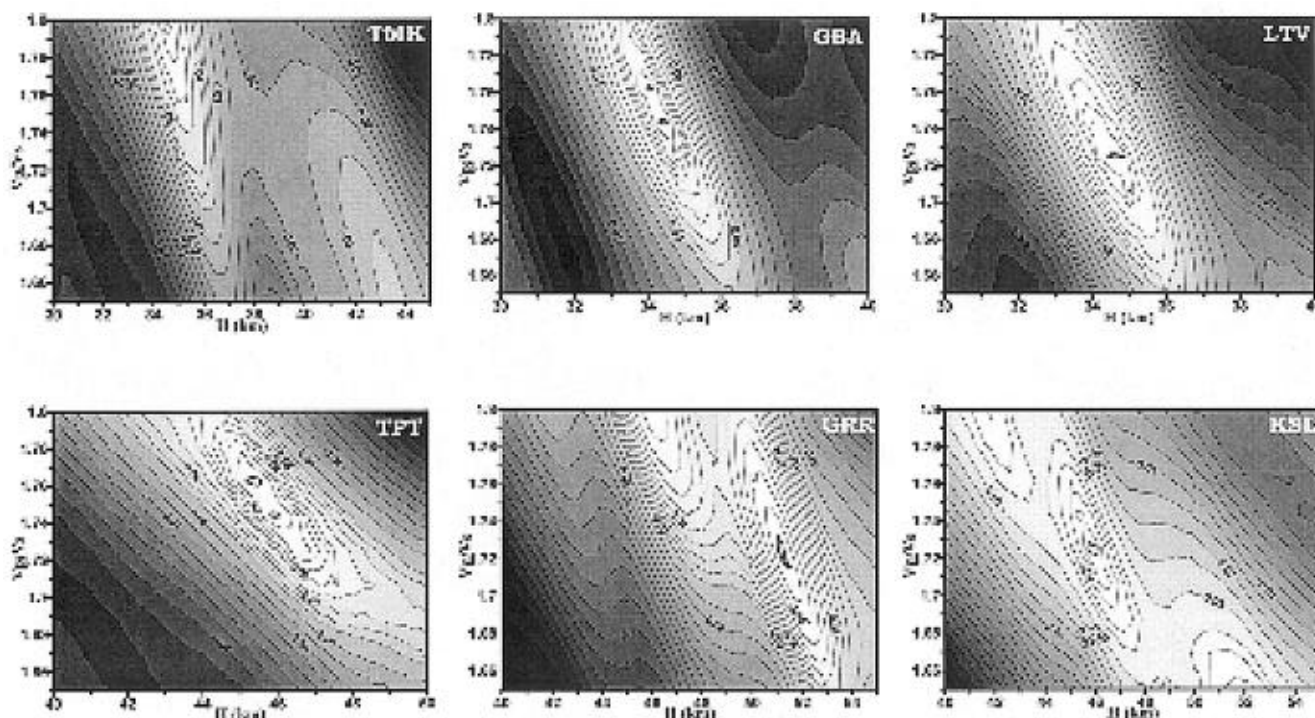


Figure 4. The V_p/V_s ratio vs crustal thickness estimate for selected stations.

Table 1. Station location, crustal thickness, V_p/V_s and Poisson's ratio

Station name	Latitude (°N)	Longitude (°E)	Elevation (m)	P_s-P (s)	Thickness (km)	V_p/V_s	Poisson's ratio (s)
Cuddapah basin (CB)							
SLM	16.10	78.89	368	4.07	34.5–33.5	1.73–1.77	0.25–0.26
CUD	14.48	78.77	150	4.16	35.2–34.1	1.74–1.78	0.25–0.26
Eastern Dharwar craton (EDC)							
MBN	16.87	77.66	417	4.00	34.8–33.9	1.71–1.74	0.24–0.25
LTV	14.93	77.28	402	4.08	35.3–33.5	1.71–1.77	0.24–0.26
KDR	14.18	78.16	453	4.55	39.5–40.3	1.71–1.72	0.23–0.25
KOL	12.95	78.25	803	3.92	33.8–33.0	1.72–1.77	0.25–0.26
BGL	13.02	77.57	791	4.07	35.2–34.6	1.73–1.74	0.25–0.26
GBA	13.56	77.36	681	4.10	34.9–33.4	1.73–1.78	0.25–0.26
Closepet granite (CG)							
TMK	13.34	77.19	842	4.49	35.0–34.2	1.78–1.80	0.27–0.28
Chitradurga thrust (CT)							
NTR	13.30	76.90	712	4.72	41.4–40.8	1.73–1.74	0.25–0.26
KBC	13.30	76.65	763	4.90	42.5–41.3	1.71–1.74	0.24–0.25
Western Dharwar craton (WDC)							
TPT	13.27	76.54	785	5.43	46.1–45.4	1.74–1.76	0.25–0.26
DHR	15.43	74.98	679	5.54	43.5–42.4	1.78–1.80	0.27–0.28
CRP	13.02	76.32	824	5.60	45.0–43.7	1.75–1.78	0.26–0.27
GRR	12.83	76.06	792	5.91	51.9–50.8	1.70–1.74	0.24–0.25
KSL	12.49	75.91	796	5.47	46.3–45.5	1.75–1.72	0.25–0.26

Crustal cross-section

To study the correlation of Moho depth variation with surface geology, we present a crustal cross-section from KSL to CUD (Figure 5). Moho depth is computed at indi-

vidual station due to events from SW-W, NE-E and total. The depths are projected with horizontal offset in the direction of earthquake. The crustal thickness varies between 33 and 40 km beneath EDC in contrast with 43–52 km over WDC. To examine the possibility that these

Moho depth variations could be due to dip, we also looked into receiver functions at individual station with varying distance and azimuth. No significant variation was observed in converted and multiples amplitude and arrival time as expected for a dipping Moho. We, therefore, conclude that Moho is essentially horizontal and offsets are sharp boundaries. The crustal thickness estimate for the late-Archean eastern Dharwar craton is similar to the global average (30–40 km). The mid-Archean nucleus in western Dharwar craton is, however, considerably (> 10 km) thicker than that of an average Archean shield. The other Archean terrains with significant crustal thickness (45–50 km) include Kapuskasing structural zone²⁷, Minnesota River Gneiss terrain²⁸ and Wyoming Province²⁹. All these terrains have been subjected to extensive reworking in Proterozoic unlike WDC where the crustal evolution is primarily during mid-Archean (3.4–3.0 Ga) and lacks geological signatures of subsequent tectonic perturbations. The contact between EDC and WDC is observed as gradational between the western edge of Closepet granite and Chitradurga thrust where crustal thickness changes by at least 6 km. It is interesting that this zone is also characterized by three east-dipping reflectors inferred from DSS measurements²². At station KDR, on the south-western edge of Cuddapah basin (CB), we observed crustal thickening of 5 km relative to both EDC and CB. The remarkable spatial correlation of observed crustal thickening with 1.8 Ga volcanics in this region requires detailed modelling of the wave-form at KDR.

Teleseismic residual and lithospheric thickness

Seismological data suggest strong correlation between upper mantle shear velocity and crustal type. The continents show decrease in heat flow and increase in lithospheric thickness with increasing time interval since the last major thermal or orogenic event³⁰. The mapping of

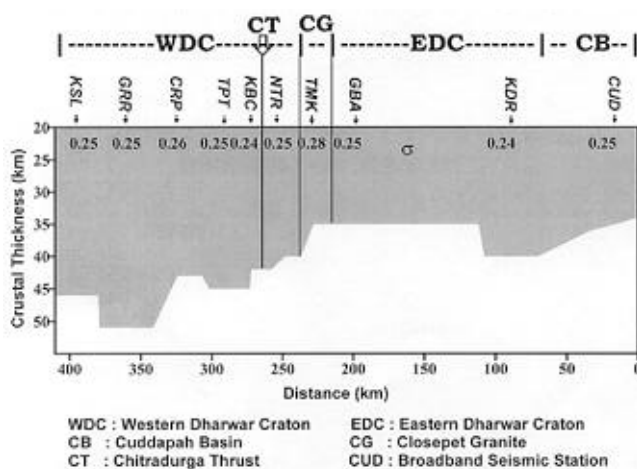


Figure 5. A west-east cross-section (from KSL to CUD) of estimated crustal thickness across the Dharwar craton. Average crustal Poisson's ratio is also depicted for individual stations.

lithospheric thickness beneath EDC and WDC could therefore suggest whether these terrains have been subsequently remobilized during Proterozoic age. A compilation of S wave travel time anomalies^{31,32} shows progressive increase in vertical travel time from a thick lithosphere craton to a thin one. We investigate the nature of lithospheric variation within the Dharwar craton using teleseismic P and S wave travel times. The predicted P and S wave arrival times were computed using IASP91 tables³³ and then subtracted from observed times to give the travel time residual. This contains the effect of crust, source mislocation, origin time error and heterogeneity along the entire path. The effect of crustal inhomogeneity is considered by computing relative travel time residuals reduced to a common depth of 52 km (maximum observed crustal thickness in EDC and WDC) assuming an average crustal $V_p \sim 6.45$ km/s, $V_s \sim 3.73$ km/s, uppermost mantle P velocity 8.2 km/s and S velocity 4.65 km/s. Other contributions to the residual is minimized by subtracting the array average from all other station residuals. The resulting relative residual represents the effect of lateral heterogeneity in the upper mantle to a depth approximately equal to the array length (~ 350 km). The relative residuals corrected for the crust for selected stations are presented in Figures 6 and 7 for earthquakes

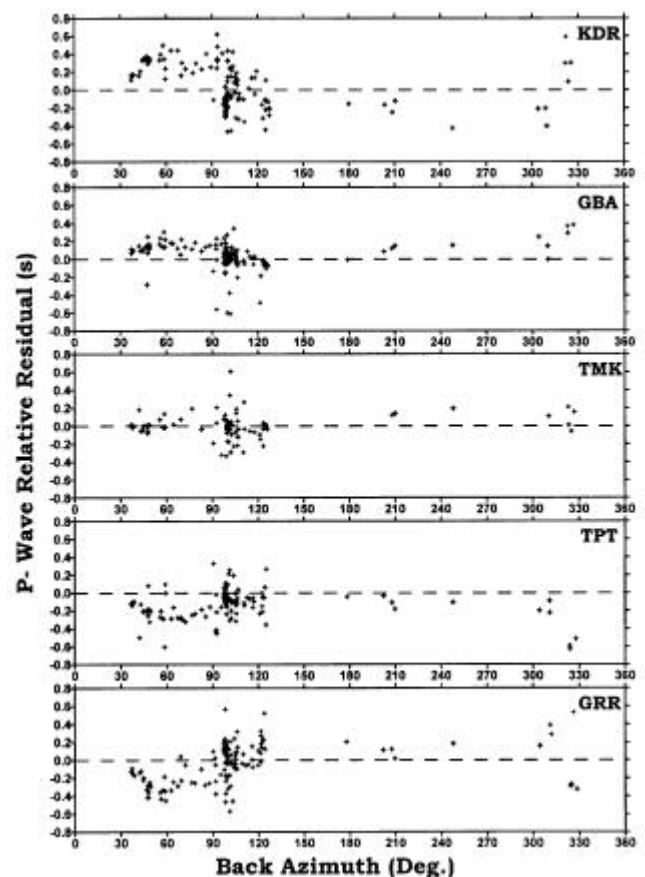


Figure 6. Azimuthal variation of crust-corrected teleseismic P-wave relative residual for selected stations.

from different azimuth ranges. Positive residuals indicate travel time delayed for rays due to its passage through a low-velocity zone while negative residual represents travel through a high-velocity region. Strong azimuthal variation indicates deep-seated causative source. It is very clear that the residuals emerge negative for stations in WDC compared to EDC representing faster arrival of seismic waves.

To examine the likely cause for systematic variation of the crust-corrected residual, we present upper mantle travel time residual across the Dharwar craton (Figures 8 a,b) for earthquakes from NE azimuth (40°–60°) coinciding with the profile along stations (KSL-GRR-TPT-TMK-GBA-KDR). For P, WDC stations have 0.3 to 0.6 s early teleseismic arrivals relative to EDC. Correspondingly, S travel time shows an average of 0.5 to 0.7 s early arrivals for WDC stations. The most likely candidate for the systematic variation of the mantle residual is the variation of depth to the base of the lithosphere. Since the data are relative residual, we can only compute relative thickness variation. The geochemical analysis of kimberlite xenoliths (1100 Ma) around LTV station in EDC constrains a minimum of 200 km thick lithosphere beneath the EDC during Proterozoic³⁴. Using a 0.5 km/s P-wave

velocity contrast between lithosphere and asthenosphere, we observe a minimum of 60–80 km lithosphere thickening beneath the WDC as compared to EDC (Figure 8 c). This supports the view that older continents have thicker and rigid root than the younger ones. This also implies that WDC has not been affected by any major younger tectonothermal event. This is also supported by lower heat flow of $30 \pm 4 \text{ mW m}^{-2}$ in WDC compared to $40 \pm 3.4 \text{ mW m}^{-2}$ in EDC³⁵, which gives rise to the observed S delay. Presence of a thicker and rigid lithospheric root beneath WDC could be responsible for its dynamic stability since 3.0 Ga and the preservation of its original Moho characteristic.

Conclusion/Archean crustal evolution

Analysis of teleseismic broadband wave-form from an experiment in the east and west Dharwar craton suggests distinct crustal architecture for the two terrains. The early-/mid-Archean (3.4–3.0 Ga) WDC crust is significantly thicker (43–52 km) compared to the global average of 30–40 km for Archean crust whilst the late-Archean (~ 2.5 Ga) EDC crust is 33–40 km thick similar to those

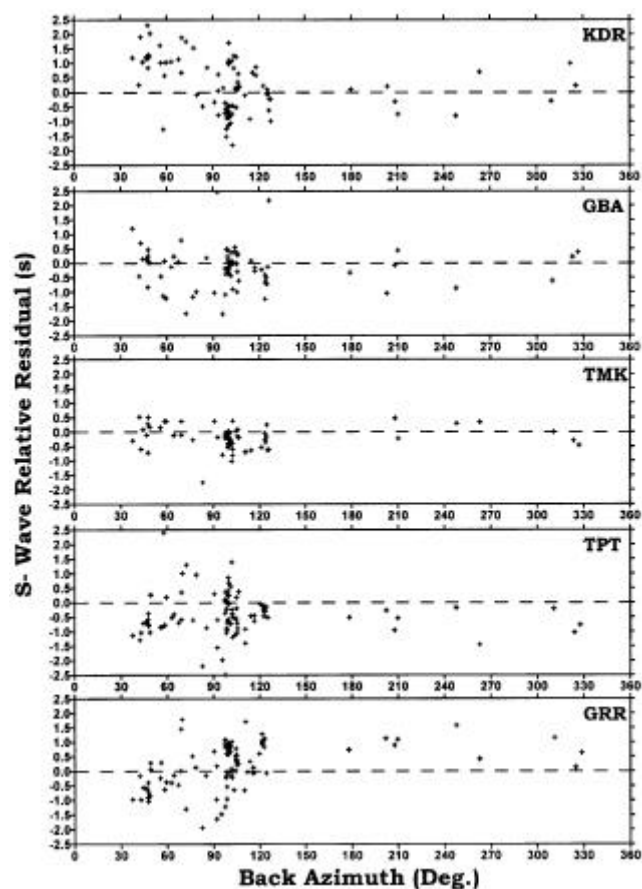


Figure 7. Azimuthal variation of crust-corrected teleseismic S-wave relative residual for selected stations.

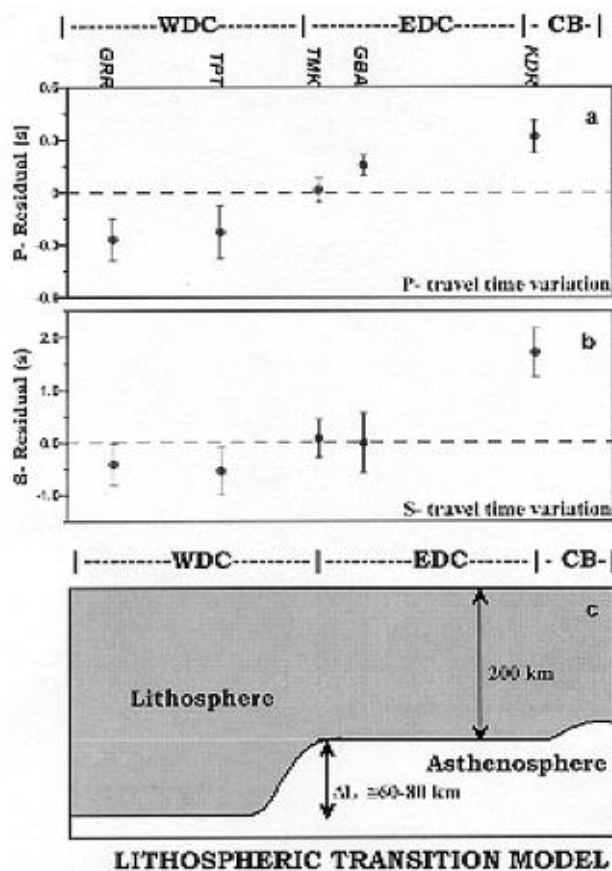


Figure 8. a, b, Mantle contribution to the teleseismic P and S residual at individual station across Dharwar craton. Time residual due to earthquakes from azimuth 40°–60° are averaged for presentations. c, Lithospheric thickness variation across Dharwar craton.

observed elsewhere. The average crustal Poisson's ratio for both EDC and WDC show similar values of 0.24–0.28, which are lower than the global average for Archean shield (0.27–0.31), suggesting felsic to intermediate composition. The thicker crust beneath WDC is also underlain by thicker lithosphere root. The crustal thickness increase causes a decrease in gravity and elevation uplift, but the increase in lithosphere thickness has opposite effect on the elevation. This explains why despite thicker crust, WDC nucleus has little topographic expression. The thicker crust beneath WDC nucleus (at GRR) is responsible for a gravity low³⁶ (– 120 mgal) observed around Gorur–Hassan region of WDC.

It is interesting to note that the overthick (52 km) crustal block coincides with the > 3.36 Ga-old Archean gneisses of Gorur–Hassan region bounded to the west and east by mid-/late-Archean shear belts. Mineral assemblages in this part of WDC represent amphibolite grade metamorphism at about 5–7 kb pressure suggesting that the Archean crust equilibrated at a depth of 15 to 25 km. Presence of these high-pressure mineral assemblages at the surface of continental crust demonstrates that the Archean crust in parts of western Dharwar craton 3.0 Ga ago must have been at least 60–80 km thick. Preservation of such an overthickened crust would only be possible in a crust shielded from high mantle heat flow by a thick, insulating layer of subcrustal lithosphere³⁷ where heat transport was by conduction rather than by convection. Presence of such a thick lithospheric root has been demonstrated in this study beneath the WDC. Thick and rigid lithosphere formed beneath the WDC during early time probably helped in preserving the primitive crustal architecture. Presence of segmented deep crustal blocks with Moho depth 38–41 km in WDC was also revealed by DSS data from Kavali–Udipi profile. Within each of these blocks, the Moho is essentially horizontal.

We speculate that the crustal blocks inferred from seismological studies and also through field geology³⁸ represent distinct Archean blocks accreted together to form WDC. Presence of the overthickened Archean crustal blocks of WDC with felsic to intermediate composition suggests that the crustal growth resembles island arc tectonic settings along the sites of plate collision. Similar overthickened crust (~ 60–80 km) with low s is also observed in Andean orogenic zone³⁹. This, however, suggests that the behaviour of mid-Archean lithosphere was also governed by the present-day plate tectonic processes. A stabilized WDC craton subsequently accreted to the EDC around 2600 Ma along Chitradurga thrust – Closepet granite. Lithospheric thicknesses show marked reduction to the east of Closepet granite. It is interesting to note that the DSS reflection survey shows prominent east dipping reflectors from Chitradurga thrust to western part of Closepet granite coinciding with our inferred gradation Moho in the zone, which may be an indication of subduction of western Dharwar craton to the east.

A detailed modelling of seismic wave-form from the broadband experiment currently in progress would soon reveal the untold complex structure and Archean geodynamics of the Dharwar craton.

1. Taylor, S. R. and McLennan, S. M., *Rev. Geophys.*, 1995, **33**, 241–266.
2. Christensen, N. I. and Mooney, W. D., *J. Geophys. Res.*, 1995, **100**, 9761–9788.
3. Rudnick, R. L. and Fountain, D. N., *Rev. Geophys.*, 1995, **33**, 267–309.
4. Durrheim, R. J. and Mooney, W. D., *J. Geophys. Res.*, 1994, **99**, 15359–15374.
5. Zandt, G. and Ammon, C. J., *Nature*, 1995, **374**, 152–154.
6. Last, R. J., Nyblade, A. A., Langston, C. A. and Owens, T. J., *J. Geophys. Res.*, 1997, **102**, 24469–24483.
7. Chevrot, S. and Van der Hilst, R. D., *Earth Planet. Sci. Lett.*, 2000, **183**, 121–132.
8. Christensen, N. I., *J. Geophys. Res.*, 1996, **101**, 3139–3156.
9. Holbrook, N. D., Mooney, W. D. and Christensen, N. I., *Continental Lower Crust* (eds Fountain, D. M., Arculus, R. and Kay, R.), Elsevier, New York, 1992, pp. 21–43.
10. Drury, S. A., Harris, N. B. N., Holt, G. J., Reeves-Smith, G. J. and Wightman, R. T., *J. Geol.*, 1984, **92**, 3–20.
11. Naqvi, S. M. and Rogers, J. J. W., *Precambrian Geology of India*, Oxford Univ. Press, 1987, p. 223.
12. Goodwin, A. M., *Principles of Precambrian Geology*, Academic Press, London, 1996, p. 327.
13. Beckinsale, R. D., Drury, S. A. and Holt, R. W., *Nature*, 1980, **283**, 469–470.
14. Meen, J. K., Rogers, J. J. W. and Fullager, P. D., *Geochim. Cosmochim. Acta*, 1992, **56**, 2455–2470.
15. Chadwick, B., Ramakrishnan, M., Vasudev, V. N. and Viswanatha, M. N., *J. Geol. Soc. London*, 1989, **146**, 825–834.
16. Krogstad, E. J., Balakrishnan, S., Mukhopadhyay, D. K., Rajamani, V. and Hansen, G. N., *Science*, 1989, **243**, 1337–1340.
17. Chatterjee, N. and Bhattacharji, S., *Proc. Indian Acad. Sci. (E & P)*, 2001, **110**, 433–453.
18. Ammon, C. J., *Bull. Seismol. Soc. Am.*, 1991, **81**, 2504–2510.
19. Zandt, G., Myers, S. C. and Wallace, T. C., *J. Geophys. Res.*, 1995, **100**, 10529–10548.
20. Zhu, L. and Kanamori, H., *J. Geophys. Res.*, 2000, **105**, 2969–2980.
21. Sarkar, D., Chandrakala, K., Padmawathi Devi, P., Sridhar, A. R., Sain, K. and Reddy, P. R., *J. Geodyn.*, 2001, **31**, 227–241.
22. Kaila, K. L. *et al.*, *J. Geol. Soc. India*, 1979, **20**, 307–333.
23. Rai, S. S., Priestley, Keith, Suryaprakasam, K., Srinagesh, D., Gaur, V. K. and Du, Z., *J. Geophys. Res.*, 2003, **108(B2)**, 2088 doi 10.1029/2002 JB 001776.
24. Kumar, M. R., Saul, J., Sarkar, D., Kind, R. and Shukla, A. K., *Geophys. Res. Lett.*, 2001, **28**, 1339–1342.
25. Newton, R. C. and Hansen, E. C., *Geol. Soc. London Spec. Pub. No. 24*, 1986, 297–308.
26. Ramachandran, C., *Tectonophysics*, 1992, **201**, 187–198.
27. Boland, A. V. and Elis, R. M., *J. Geophys. Res.*, 1989, **94**, 7189–7204.
28. Boyd, N. K., Clement, W. P. and Smithson, S. B., *EOS Trans. AGU*, 1992, **73**, 354–355.
29. Mooney, W. D. and Braille, L. W., *The Geology of North America* (eds Bally, A. W. and Palmer, A. R.), Mem. Geol. Soc. Am. 172, 1989, pp. 39–52.
30. Sclater, J. G., Jaupart, C. and Galson, D., *Rev. Geophys. Space Phys.*, 1980, **18**, 269–311.
31. Wickens, A. J. and Buchbinder, G. G. R., *Bull. Seismol. Soc. Am.*, 1980, **70**, 809–822.

RESEARCH ARTICLES

32. Bockelmann, G. H. R. and Silver, P. G., *J. Geophys. Res.*, 2000, **105**, 579–605.
33. Kennett, B. L. and Engdahl, E. R., *Geophys. J. Int.*, 1991, **105**, 429–465.
34. Ganguly, J. and Bhattacharya, P. K., *Petrology and Geophysical Implications in Mantle Xenoliths* (ed. Nixon, P.), Wiley and Sons, 1987, pp. 249–265.
35. Gupta, M. L., Sunder, A. and Sharma, S. R., *Tectonophys.*, 1991, **194**, 107–122.
36. National Geophysical Research Institute, Bouguer Gravity Anomaly Map of India (GPH/2), 1978.
37. Davies, G. F., *Earth Planet Sci. Lett.*, 1979, **44**, 231–238.
38. Ramakrishnan, M., *Geo Karnataka* (eds Ravindra, B. M. and Ranganathan, N.), Dept. of Mines and Geology, Bangalore, 1994, pp. 6–35.
39. Beck, S. L., Zandt, G., Meyers, S. C., Wallace, T. C., Silver, P. G. and Drake, L., *Geology*, 1996, **24**, 407–410.

ACKNOWLEDGEMENTS. The study is funded by the Department of Science & Technology program on Deep Crustal Studies. SSR is grateful to Prof. D. Mukhopadhyay and Dr R. Srinivasan for their insight and help over many years in understanding the geology of Dharwar craton. This is a part of the Ph.D. work of Sandeep Gupta.

Received 31 May 2002; revised accepted 16 December 2002
